

# Fabrication and characterization of low loss rib chalcogenide waveguides made by dry etching

Yinlan Ruan, Weitang Li, Ruth Jarvis, Nathan Madsen,  
Andrei Rode, Barry Luther-Davies

Center for Ultra-high-bandwidth Devices for Optical Systems and Australian Photonics Cooperative Research  
Center, Laser Physics Center, The Australian National University, Canberra 0200 Australia  
[lan111@rsphysse.anu.edu.au](mailto:lan111@rsphysse.anu.edu.au)

**Abstract:** We report the fabrication and characterization of rib chalcogenide waveguides produced by dry etching with  $\text{CF}_4$  and  $\text{O}_2$ . The high index contrast waveguides ( $\Delta n \sim 1$ ) show a minimum propagation loss of 0.25 dB/cm. The high refractive nonlinearity of  $\sim 100$  times silica in  $\text{As}_2\text{S}_3$  allowed observation of a  $\pi$  phase shift due to self-phase modulation of an 8 ps duration 1573 nm pulse in a 5 cm long waveguide.

©2004 Optical Society of America

OCIS codes: (230.7370) Waveguides; (250.5300) Photonic integrated circuits.

---

## References and links

1. T. Cardinal, K. A. Richardson, H. Shim, A. Schulte, R. Beatty, K. Le Foulgoc, C. Meneghini, J. F. Viens, and A. Villeneuve, "Non-linear optical properties of chalcogenide glasses in the system As-S-Se," *J. Non-Cryst. Solids*, **256-257**, 353-360 (1999).
2. J. T. Gopinath, M. Soljacic, E. P. Ippen, V. N. Fuflyigin, W. A. King, and M. Shurgalin, "Third-order nonlinearities in  $\text{Ge}_{33}\text{As}_{12}\text{Se}_{55}$  glass for high-index contrast fiber devices," in Proceedings of 2004 Conference on Lasers and Electro-optics/International Quantum Electronics Conference, (USA,2004), pp. CFA3.
3. R. E. Slusher, and B. J. Eggleton, "Chalcogenide glasses," in *Nonlinear Photonic Crystals*, R. E. Slusher, B. J. Eggleton, ed. (Springer, 2003).
4. C. B. Pedroso, E. Munin, A. B. Villaverde, J. A. Medeiros Neto, N. Aranha, and L. C. Barbosa, "High Verdet constant Ga:S:La:O chalcogenide glasses for magneto-optical devices," *Opt. Eng.*, **38**(2), 214-219 (1999).
5. C. C. Huang, D. W. Hewak, and J. V. Badding, "Deposition and characterization of germanium sulphide glass planar waveguides," *Opt. Express*, **12**, 2501-2506 (2004), <http://www.opticsexpress.org/abstract.cfm?URI=OPEX-12-11-2501>
6. J-F. Viens, C. Meneghini, A. Villeneuve, T. V. Galstian, E. J. Knystautas, M.A. Duguay, K.A. Richardson, and T. Cardinal, "Fabrication and characterization of integrated optical waveguides in sulphur chalcogenide waveguide," *J. Lightwave Technol.*, **17**(7), 1184-1191 (1999).
7. S. Ramachandran, and S.G. Bishop, "Excitation of  $\text{Er}^{3+}$  emission by host glass absorption in sputtered films of Er-doped  $\text{Ge}_{10}\text{As}_{40}\text{Se}_{25}\text{S}_{25}$  glass," *Appl. Phys. Lett.*, **73**, 3196 (1998).
8. S. Spalter, H. Y. Hwang, J. Zimmermann, G. Lenz, T. Katsufuji, S-W. Cheong, and R.E. Slusher, "Strong self-phase modulation in planar chalcogenide glass waveguide," *Opt. Lett.*, **27**(5), 363-365 (2002).
9. A. V. Rode, A. Zakery, M. Samoc, R.B. Charters, E.G. Gamaly, and B. Luther-Davies, "Laser-deposited  $\text{As}_2\text{S}_3$  chalcogenide films for waveguide applications," *Appl. Surf. Sci.*, **197-198**, 481-485 (2002).
10. A. J. Perry, D. Vender, and R.W. Boswel., "The application of the helicon source to plasma processing," *J. Vac. Sci. Technol.*, **B**, **9**(2), 310-317 (1991).
11. G. P. Agrawal, "Self-phase modulation," in *Nonlinear Fiber Optics*, P.L. Kelley, I. P. Kaminow, G. P. Agrawal, ed. (Academic, 2001).
12. Y. Ruan, B. Luther-Davies, W. Li, A. Rode, and M. Samoc, "Nonlinear integrated optical waveguides in chalcogenide glasses," *ACTA Optica Sinica*, **23** (Supplement 363), 363-364 (2003).
13. Y. Ruan, B. Luther-Davies, M. Samoc, A. Rode, R. Jarvis, and Steve Madden, "The dispersion of the third order nonlinearities in chalcogenide glasses and rib waveguides," to be published.
14. M. Asobe, T. Kanamori, K. Naga Numa, and H. Itoh, "Third-order nonlinear spectroscopy in  $\text{As}_2\text{S}_3$  chalcogenide glass fibers," *J. Appl. Phys.*, **77**(11), 5518-5523 (1995).
15. T. Shoji, T. Tsuchizawa, T. Watanabe, K. Yamada, and H. Morita, "Low loss mode size converter from 0.3 $\mu\text{m}$  square Si wire waveguides to single mode fibers," *Electron. Lett.* **38**(25), 1669-1670 (2002).

## 1. Introduction

The third order nonlinearity of an optical material can be used for fast all-optical processing in optical fibre networks including all-optical multiplexing and de-multiplexing; wavelength conversion; Raman and parametric amplification. Chalcogenide glasses were reported to have third nonlinear refractive indexes more than 500 times higher than fused silica with similar response times and good figures of merit [1-3]. Furthermore, chalcogenides form glasses over a wide range of compositions, allowing their refractive indexes to be tuned to create almost arbitrarily high index contrast between the core and cladding. This allows single mode waveguides with small cross-sectional area and small bend radii to be fabricated. As a result of these physical characteristics, the peak power for all-optical processing of  $< 1$  W should be achievable in planar waveguide structures fabricated in chalcogenide glasses. The high linear index also allows structures incorporating photonic crystals to be fabricated, whilst the strong dispersion in the infra-red results in moderate Verdet constants also indicating that chalcogenides are promising for magneto-optic devices [4].

To realize the potential of chalcogenides for planar waveguide devices it is necessary to develop techniques for both fabricating low loss chalcogenide glass films and patterning them into micron-size low loss optical waveguides. Thermal evaporation, sputter deposition, chemical vapour deposition and pulsed laser deposition have all been used to produce waveguide quality films [5-7]. To date most patterning has been done using laser-writing [6,8] where waveguides are produced using the photosensitivity of most chalcogenides to light near their band edge. Typically for  $\text{As}_2\text{S}_3$ , irradiation at either 514 nm or 532 nm at fluencies around  $100 \text{ J/cm}^2$  results in an index increase up to 0.04. Unfortunately, in most cases these photo-induced changes can relax, making this method unsuitable for producing devices which are required to be stable over a long period. As a result, alternative fabrication methods are required.

Unfortunately, chalcogenide glasses are less robust, have higher thermal expansion coefficient and lower glass transition temperatures ( $T_g$ ) than oxide glasses. These physical properties inevitably increase the difficulties of fabricating micron-size structures, especially when using processes involving in wet chemistry or high temperatures. Although wet etching was used to fabricate chalcogenide waveguides [6], undercutting of the mask layer always results in slanted sidewalls, which makes the control of waveguide dimensions difficult. Recently, rib germanium sulphide waveguides were fabricated by using Ar dry etching, however, the profile of waveguides was not rectangular, which was believed to be due to the low selectivity in the etch rate between the chalcogenide film and photoresist mask [5].

In this paper, we report the fabrication of low loss chalcogenide rib waveguides made by dry etching fully compatible with mature silicon microelectronics fabrication processes. Waveguide losses as low as  $0.25 \text{ dB/cm}$  have been achieved and a phase shift  $\sim \pi$  due to self phase modulation has been obtained using a  $\sim 40 \text{ W}$  peak power pulse in a  $5 \text{ cm}$  long waveguide. The results suggest that it will be possible to reduce the switching power to  $\sim 1 \text{ W}$  for all-optical Mach-Zehnder interferometer.

## 2. Waveguide fabrication

### 2.1 Sample preparation

The chalcogenide glasses used in our experiments included  $\text{As}_2\text{S}_3$ ,  $\text{As}_{40}\text{S}_{45}\text{Se}_{15}$ ,  $\text{As}_{24}\text{S}_{38}\text{Se}_{38}$  and  $\text{Ge}_{33}\text{As}_{12}\text{Se}_{55}$ .  $\text{As}_2\text{S}_3$  and  $\text{Ge}_{33}\text{As}_{12}\text{Se}_{55}$  glasses were obtained from Amorphous Materials Inc.  $\text{As}_{40}\text{S}_{45}\text{Se}_{15}$  and  $\text{As}_{24}\text{S}_{38}\text{Se}_{38}$  samples were prepared in collaboration with researchers at the University of Central Florida. Thin films were prepared from the bulk samples using Ultra-Fast Pulsed Laser Deposition (UFPLD) which employed a frequency doubled mode-locked Nd:YAG laser producing  $6 - 7 \text{ W}$  average power ( $70 - 80 \text{ nJ/pulse}$ ) at  $532 \text{ nm}$ , at a repetition rate of  $76 \text{ MHz}$  [9]. The substrates were silicon wafer covered with a  $2.4 \mu\text{m}$  thermal oxide layer to act as a buffer to isolate the field from the Si substrate. UFPLD has been demonstrated to produce atomically smooth films in chalcogenide glasses free from

particle contamination. Furthermore, the surface layer of the target is ablated with moderately high kinetic energy which helps to densify the resulted films and to remove the need to anneal films prior to waveguide processing.

Standard photolithography techniques were used to prepare an Al mask prior to dry etching. It was found necessary to coat the chalcogenide with a thin layer (200 nm) of photoresist prior to sputtering the Al mask layer. This thin photoresist layer avoided the formation of bubbles at the metal-chalcogenide interface. Dry etching systems employed in this work were either a helicon plasma source which had been described in earlier publications [10] or an Oxford Instruments RIE-100 ICP etcher. The high ion density and low plasma potential was used to etch samples with independently controllable RF power and substrate bias voltage.

## 2.2 Helicon plasma etching

When etching using the helicon system, the RF power was fixed at 600 W in order to achieve enough high density plasma whilst the gas ratio and bias voltage were varied and optimized. It was observed that  $\text{CF}_4$  gas alone etched the chalcogenide films slowly but the etch rate could be markedly increased using a  $\text{CF}_4/\text{O}_2$  gas mixture. Both the substrate bias voltage and the gas ratio were found to affect the sidewall angle. To achieve vertical sidewalls it was found to be necessary to increase the substrate bias as the content of heavy Se atom in Se-based glasses increased. The optimal parameters to obtain structures as shown in Fig. 1(a) were RF power 600 W,  $\text{CF}_4/\text{O}_2$  ratio 14.3%, and substrate bias voltage 130 to 160 V. The etch rate of  $\text{As}_2\text{S}_3$  waveguides was about 250 nm/min.

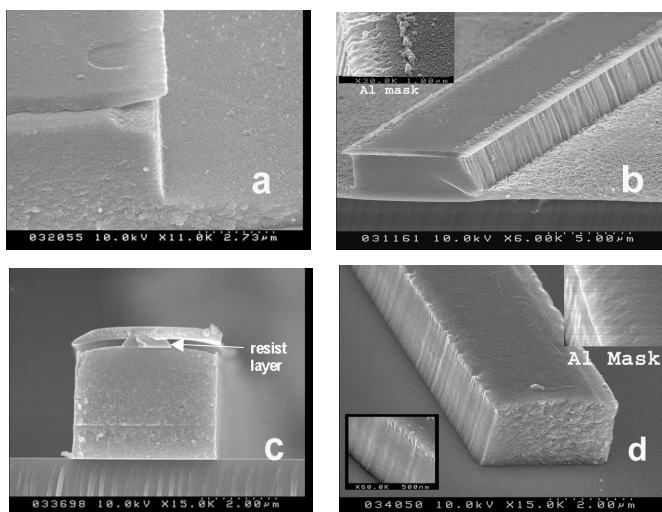


Fig. 1. SEM images showing the profile of  $\text{As}_2\text{S}_3$  waveguides etched by helicon plasma using Al masks (a) showing vertical sidewall but corner damage resulted from weak adhesion between Al and  $\text{As}_2\text{S}_3$  layer; (b) rough Al mask resulted in rough waveguide sidewall; (c) the cross-section showing smooth corner by inserting a thin photoresist layer; (d) smooth Al mask as well as vertical and smooth waveguide sidewall.

Once vertical sidewalls had been obtained it became necessary to improve the smoothness of the sidewall to reduce the optical losses. It can be seen from Fig. 1(b) that the Al mask played a crucial role because etching of underlying layer directly mirrored any structure in the mask.  $\text{O}_2/\text{Ar}$  plasma and acid pre-treatments of the top surface of Al films were used to improve the adhesion of the upper photoresist layer and this reduced the roughness of the mask as shown in Fig. 1(d).

Corner damage to the waveguides was also observed in some conditions as shown in Fig. 1(a), and was resulted from weak adhesion between the chalcogenide film and the Al layer. This problem existed in spite of plasma pre-treatment of the chalcogenide layers prior to Al

deposition and patterning, and could be traced to the formation of bubbles at the chalcogenide-Al interface mentioned earlier. The thin photoresist layer between the Al and chalcogenide film was effective in eliminating this problem as shown in Fig. 1(c).

As<sub>2</sub>S<sub>3</sub> waveguides with vertical and relatively smooth sidewall (peak-to-peak roughness was estimated to be < 50 nm from its SEM image) was obtained and shown in Fig. 1(d). This sidewall roughness was low enough to obtain moderate scattering losses even when using high index contrast ( $n \approx 1@1.55 \mu\text{m}$ ) provided the waveguide width was  $\geq 3 \mu\text{m}$ . During plasma etching the waveguides decreased in width by 0.3-0.7  $\mu\text{m}$  relative to the mask width due to undercutting, making control of the width of the smallest structures difficult.

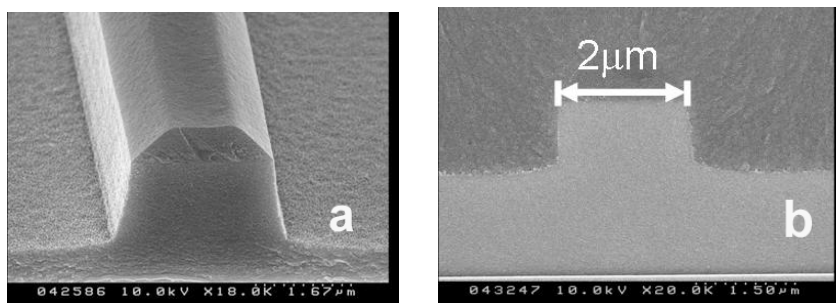


Fig. 2. SEM micrographs showing the profile of As<sub>2</sub>S<sub>3</sub> waveguides etched by ICP using photoresist mask (a) As<sub>2</sub>S<sub>3</sub> waveguide with photoresist mask (b) coating with polysiloxane cladding, its width is well controlled as required.

### 2.3 ICP etching

We also successfully applied the Oxford Instruments RIE-100 ICP system to etch chalcogenide waveguides. Our experiments indicated that the high density ICP plasma etcher resulted in very similar etching behaviour to the helicon plasma etcher. However, the etching rate for the chalcogenide glasses was about an order of magnitude higher when using the same RF power and bias voltage, whilst the etch rate of the photoresist was unchanged, indicating that a better selectivity was obtained between the photoresist and the chalcogenide films. This improved selectivity made it possible to eliminate the Al layer and use the photoresist alone as the mask. An As<sub>2</sub>S<sub>3</sub> waveguide etched by the ICP system using a photoresist mask is shown in Fig. 2(a). In this case the waveguide width was almost identical to the mask width as, for example, shown in Fig. 2(b) where the mask width was 2  $\mu\text{m}$ . Thus it proved easier to obtain narrower waveguides and to control their width and profile using the ICP etcher, whilst elimination of the metal mask simplified the pattern transfer process.

## 3. Experimental characterization

### 3.1 Loss measurement

A number of chalcogenide rib waveguides with structure shown in Fig. 3(a) were fabricated with width,  $a$ , ranging from 1 to 7  $\mu\text{m}$  and etch depth,  $b$ , from 0 to 4  $\mu\text{m}$ . A high quality polysiloxane coating ( $n = 1.53@1.55 \mu\text{m}$ ) was applied to the top of waveguides as a cladding during characterization. Propagation loss measurements were performed using the cut-back method using waveguides of lengths between 12 and 50 mm. The high index contrast ensured that light was tightly confined in the core layer. A high numerical aperture (NA) fiber with mode field diameter of 4.2  $\mu\text{m}$  at 1.55  $\mu\text{m}$  wavelength was used as input and output fiber to reduce the mode mismatch to the waveguides. The loss of waveguides with  $a = 3, 4, 5 \mu\text{m}$ ,  $b = 1.8 \mu\text{m}$  and  $c = 2.5 \mu\text{m}$  were characterized in detail.

Although the simulation showed that these deeply-etched waveguide structures supported multiple modes at 1.31  $\mu\text{m}$  and 1.55  $\mu\text{m}$ , higher order modes generally have high losses due

to the stronger coupling of the propagating field to the sidewalls. As a result, only the fundamental mode shown in Fig. 3(b) was observed to propagate along these waveguides.

Linear fitting of the measurements of the transmission coefficient as a function of the length as shown in Fig. 3(c), gave the smallest loss of 0.25 dB/cm at 1550 nm for the 4 and 5  $\mu\text{m}$  wide waveguides, increasing to about 0.5 dB/cm for the 3  $\mu\text{m}$  wide guides. This is due to the increased coupling of the fundamental mode to the sidewall as the waveguide becomes narrower. The polarization dependent loss between TE and TM modes was about 0.4 dB. Se-based chalcogenide waveguides with similar dimension were also characterized, and higher loss (1.6 dB/cm) was however found at 1550 nm. The reasons for high losses are being investigated and it could be resulted from excess absorption losses in these samples.

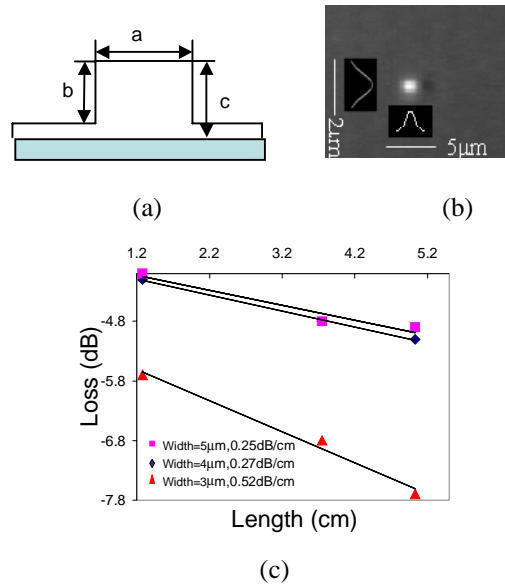


Fig. 3. (a) rib waveguide structure; (b) the output mode from  $\text{As}_2\text{S}_3$  rib waveguide with  $a=4.2$ ,  $b=1.8$ , and  $c=2.7$   $\mu\text{m}$  showing single mode propagation; (c) light transmission as a function of the waveguide length at 1550 nm.

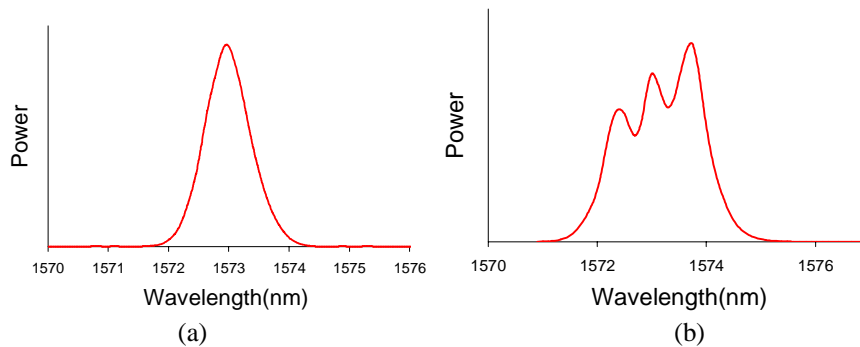


Fig. 4. (a) Spectrum of input signal at 1573 nm; (b) spectral broadening corresponding to  $\pi$  phase shift and peak power 40 W in the waveguide

### 3.2 Observation of self-phase modulation and determination of nonlinearity

To test the nonlinear properties of the chalcogenide waveguides, we measured spectral broadening due to self-phase modulation for pulses propagating through a 50 mm long and 5  $\mu\text{m}$  wide  $\text{As}_2\text{S}_3$  waveguide. As shown in Fig. 4(a), the 8 ps duration input pulses at 1573 nm were nearly transform-limited and were obtained from a KTP optical parametric oscillator

(OPO). The power from the OPO was coupled into a SMF-28 single-mode fiber with a 3 mm long section of high NA fiber thermally expanded and spliced to its output end. The use of this short length of high NA fiber allowed high peak power to be delivered to the chalcogenide waveguide without any fibre-induced phase shift. A standard SMF-28 fiber was employed to collect a small fraction of the transmitted light and couple it to an optical spectrum analyzer. The measured spectral broadening shown in Fig. 4(b) indicates that a phase shift  $\sim \pi$  was obtained [11]. The slight asymmetry in the output spectrum was due to asymmetry in the input pulse from the OPO. The peak pulse power in the waveguide was obtained from the average power delivered from the high NA fibre after correction of the coupling loss (about 1.8 dB/cm for one end) and waveguide loss, and was estimated to be 40 W. The effective area of the fundamental mode of the waveguide was modeled using a C2V Olympios mode solver and found to be  $\sim 8 \mu\text{m}^2$ . The calculated third-order nonlinearity based on the nonlinear phase shift was  $3.05 \times 10^{-18} \text{ m}^2/\text{W}$ , very close to the value of  $2.92 \times 10^{-18} \text{ m}^2/\text{W}$  measured by z-scan technique for bulk samples of the glasses [12,13]. It should be noted that our z-scan measurements of the third order optical nonlinearity for  $\text{As}_2\text{S}_3$  [12] indicate that the nonlinear figure of merit ( $T = \beta\lambda/n_2$  where  $\beta$  is the two-photon absorption coefficient) is  $< 0.1$  at 1550 nm. It is consistent with the data of reference [14] where  $T = 0.009$ , and hence two-photon absorption is expected to be negligible in these experiments [3].

From these results one can estimate the parameters required to achieve watt level switching in typical nonlinear devices such as a Mach-Zehnder interferometer which requires a nonlinear phase shift of  $\pi$ . The optical nonlinearity can be increased by a factor of 4 – 5 by choosing one of the higher nonlinearity glasses such as  $\text{Ge}_{33}\text{As}_{12}\text{Se}_{55}$ . Assuming that the optical losses of 0.2 dB/cm can be achieved in a 4  $\mu\text{m}$  wide waveguide, then  $\sim 1$  W switching power requires a 25 cm long waveguide, which could be conveniently fabricated as an 11-turn 7 mm diameter coil. Alternatively by reducing the sidewall roughness, it should be possible to shrink the waveguide cross section to  $\sim 1 \times 1 \mu\text{m}^2$ , and hence achieve an order of magnitude reduction in mode area in one of the higher nonlinearity glasses whilst still keeping the similar waveguide loss. Thus, sub-watt switching can be achieved in a 5 cm long structure, assuming that the coupling loss can be held  $< 1$  dB by using waveguide tapers [15].

#### 4. Conclusion

In conclusion, we have successfully fabricated and characterized chalcogenide waveguides by using a dry etching process. Waveguide losses as low as 0.25 dB/cm were achieved. Combining the high nonlinearity of the chalcogenides we demonstrate that it is possible to realize all-optical processing with chalcogenide waveguides and  $\sim 1$  W peak switching power.

#### Acknowledgments

The authors would like to thank RPO Pty Ltd for providing access to the Karl Suss MA6 Mask aligner used for pattern transfer and Dr Kathleen Richardson and Mr Cedric Lopez from the University of Central Florida for supplying samples of As-S-Se glasses. We also thank Mrs. Maryla Krolikowska for her assistance on sample preparation. The support of the Australian Research Council through its Federation Fellow and Centre of Excellence program is gratefully acknowledged.